JOURNAL OF CLINICAL MICROBIOLOGY, Oct. 2006, p. 3557–3561 Vol. 44, No. 10
0095-1137/06/$08.00+0 doi:10.1128/JCM.00713-06

Preparation of His-Tagged Armored RNA Phage Particles as a Control for Real-Time Reverse Transcription-PCR Detection of Severe Acute Respiratory Syndrome Coronavirus

Yangjian Cheng,[1] Jianjun Niu,[2] Yongyou Zhang,[1] Jianwei Huang,[2] and Qingge Li[1,3]*

Key Laboratory of Cell Biology and Tumor Cell Engineering of the Ministration of Education, Molecular Diagnostics Laboratory, Department of Biomedical Sciences and School of Life Sciences, Xiamen University,[1] Xiamen Center for Disease Control and Prevention,[2] and Key Laboratory of Chemical Biology of Fujian,[3] Xiamen, Fujian 361005, China

Received 5 April 2006/Returned for modification 2 June 2006/Accepted 24 July 2006

Armored RNA has been increasingly used as both an external and internal positive control in nucleic acid-based assays for RNA virus. In order to facilitate armored RNA purification, a His_6 tag was introduced into the loop region of the MS2 coat protein, which allows the exposure of multiple His tags on the surface during armored RNA assembly. The His-tagged armored RNA particles were purified to homogeneity and verified to be free of DNA contamination in a single run of affinity chromatography. A fragment of severe acute respiratory syndrome coronavirus (SARS-CoV) genome targeted for SARS-CoV detection was chosen for an external positive control preparation. A plant-specific gene sequence was chosen for a universal noncompetitive internal positive control preparation. Both controls were purified by Co^{2+} affinity chromatography and were included in a real-time reverse transcription-PCR assay for SARS-CoV. The noncompetitive internal positive control can be added to clinical samples before RNA extraction and enables the identification of potential inhibitive effects without interfering with target amplification. The external control could be used for the quantification of viral loads in clinical samples.

External positive controls (EPC) and internal positive controls (IPC) are important components in nucleic acid-based testing. An EPC is used to validate or calibrate the established assays, while an IPC is employed to reveal potential inhibition (5, 13, 15, 16, 20, 25). Ideally, both controls should closely resemble the target of interest so as to track the entire process of the assay, including pathogen lysis, nucleic acid extraction, RNA reverse transcription (RT), amplification, and detection. These controls should also be stable for long-term storage and safe for routine use. Currently used positive controls, such as pure plasmids or naked RNA, cannot fulfill these requirements. In RT-PCR particularly, naked RNA fragments are too labile, whereas plasmid DNA, although more stable than RNA fragments, is not representative of an authentic template in the RT procedure (6).

Engineered phages are good alternatives for control preparations and have been successfully used to prepare nuclease-resistant RNA positive controls, armored RNA (AR), for RT-PCR assays (4, 17, 18, 24), as well as DNA positive controls (lambda phage DNA) for PCR assays (22). The advantages of phage controls include safety, stability, and physical characteristics that mimic the natural virus. Due to the extreme lability of RNA, AR controls have been widely used (2, 3, 8, 9, 14). Unfortunately, only a limited number of AR controls are commercially available so far. Most of the commercial ARs are of little assistance to researchers, since they often use target sequences of their own, which requires customer preparation of special AR. The lack of safe and stable RNA controls could become a serious problem in cases of newly emerging pathogens such as severe acute respiratory syndrome coronavirus (SARS-CoV), where cross-infection could happen during sample exchange between laboratories (3). Therefore, there is an urgent need for a simple and straightforward preparation method for AR of various species.

AR is an engineered MS2 phage assembly that encapsulates an RNA fragment of a target gene after expression in *Escherichia coli*. Residual plasmid DNA contamination could seriously compromise its quality and performance. The major problem existing in the current AR preparation is its purification procedure. The current AR purification method involves the combined use of gradient ultracentrifugation and column chromatography (17). Despite that, the procedure is expensive and labor-intensive and has no quality control for DNA contamination (17). In order to solve such problems, we attempted to construct a recombinant plasmid for the expression of AR harboring an affinity tag at the surface of the MS2 phage assembly, and we expected that AR could be purified in a single step of affinity chromatography. Recently, MS2 was proposed as a scaffold for the display of short peptides on its surface (19, 23). The coat protein gene was modified to enable the insertion of DNA at the central part of the β-hairpin loop. Upon expression of the recombinant gene in *E. coli*, the MS2 coat protein subunits self-assemble into capsids, each comprising 180 copies of the monomer coat protein. We reasoned that a His_6 tag might also be displayed on the MS2 surface without affecting either the packing or the interaction at the protein-RNA interface, which would enable a simple, rapid purification by affinity chromatography. AR expression was thus modified and was used to prepare one EPC and one IPC for

* Corresponding author. Mailing address: Department of Biomedical Sciences, Xiamen University, South Road of Siming 422, Xiamen 361005, China. Phone: 86-592-2182100. Fax: 86-592-2187363. E-mail: qgli@xmu.edu.cn.

SARS-CoV. Both EPC and IPC could be easily purified by affinity chromatography, proved to be of homogeneous purity, and were successfully used in real-time RT-PCR detection of SARS-CoV.

MATERIALS AND METHODS

Preparation of His-tagged AR. The MS2 maturase and coat protein gene were obtained by RT-PCR from MS2 RNA (Roche, Germany) using the following primer pair: 5′-CCTTTCGGGGTCCTGCTCAACTT-3′ and 5′-GATTAGATCTGAGTTGAACTTCTTTGTTGTCTTC-3′ (the underlined sequence is a BglII restriction site). The DNA fragment was then digested with restriction enzymes BglII and NcoI and ligated with linearized pSE380 (Invitrogen, Shanghai, People's Republic of China) to generate vector pAR-1 (9). One region that covers all binding regions of the detection primers recommended by the WHO and the Chinese CDC in 2003 was selected for preparation of SARS-CoV EPC. The DNA fragment (positions 15270 to 15628) (gi 30271926) was obtained by RT-PCR from SARS-CoV RNA using primer pair 5′-GATTAGATCTCTAACATGCTTAGGATAATGG-3′ (positions 15250 to 15270) and 5′-GATTGGTACCAAATGTTTACGCAGGTAAGCGTAAAA-3′ (positions 15603 to 15628) (the underlined sequences are BglII and PstI restriction sites, respectively, throughout this paragraph). For the IPC preparation, a 125-bp-long plant-specific ribulose-1,5-bisphosphate carboxylase small subunit (*rbcs*) gene fragment was selected and obtained by PCR from *spinach* DNA using primer pair 5′-GATTGGTACCCGGTCGTTACTGGACAATGTG-3′ and GATTGGTACCCGAATCCAATGATACGGATGAA-3′. Each DNA fragment described above was verified by direct DNA sequencing before digestion with BglII and PstI and insertion into linearized pAR-1.

The His tag sequence was inserted into the above-described vectors by introducing a KpnI restriction site between codons 15 and 16 of the coat protein using a site-directed mutagenesis method (11). The synthesized His tag adaptor (5′-PO_4-GTACCCATCACCATCACCATCACG-3′/5′-PO_4-GTACCGTGATGGTGATGGTGATGG-3′) was annealed, cleaved with KpnI, and then ligated into the KpnI-cleaved vectors.

After verification by DNA sequencing, the newly generated recombinant plasmid was transformed into *Escherichia coli* strain DH5α, and protein expression was induced with 1 mM isopropyl-L-thio-D-galactopyranoside (IPTG) at 37°C for 16 h. The production of AR was detected by nondenaturing agarose gel electrophoresis before purification. Briefly, after induction, cells were collected by centrifugation and lysed by ultrasonic disruption. After a brief centrifugation (10,000 × *g* for 10 min), the supernatant (20 μl) was incubated with 2 U DNase I and/or 100 U RNase A at 37°C for 4 h. The product was checked by agarose gel electrophoresis (1%), with the gel stained with ethidium bromide.

The intact AR was inspected by HITACHI (Tokyo, Japan) H-600 transmission electron microscopy (TEM) following negative staining with 1% phosphotungstic acid.

Purification of His-tagged AR. His-tagged AR was purified with TALON metal affinity resin (Clontech Laboratories, Inc., CA) from bacterial lysates according to the manufacturer's instructions. Briefly, a total volume of 100 ml of induced bacterial culture was collected by centrifugation and then resuspended in cold lysis buffer (50 mM NaH_2PO_4, 300 mM NaCl, 15 mM imidazole, pH 8.0). After ultrasonic disruption to break cells and centrifugation to remove cell debris, the supernatant was mixed with the resin preequilibrated with lysis buffer. The resin was applied to the column after incubation for 30 min at 4°C. The column was washed with washing buffer (50 mM NaH_2PO_4, 300 mM NaCl, 30 mM imidazole, pH 8.0) until the absorption of the eluent decreased to 0.01 or less. The elution buffer (50 mM NaH_2PO_4, 300 mM NaCl, 200 mM imidazole, pH 8.0) was then applied to elute the His-tagged AR. The eluent was dialyzed against 10 mM Tris-HCl (pH 7.5) containing 100 mM NaCl and 1 mM EDTA for 12 h at room temperature with three buffer changes. To monitor each step of the purification procedure, different fractions were analyzed by sodium dodecyl sulfate-polyacrylamide gel electrophoresis (SDS-PAGE). The purified AR was also analyzed by matrix-assisted laser desorption ionization–time of flight mass spectrometry (MALDI-TOF MS) (BiflexIII; Bruker Daltonik GmbH, Bremen, Germany).

For comparison, both tagged and untagged AR were also purified using sucrose density gradient centrifugation. After induction, 100 ml of bacterial culture was collected by centrifugation and resuspended in 5 ml of lysis buffer (50 mM Tris-HCl, 5 mM $MgSO_4$, 100 mM NaCl, pH 8.0). Cells were lysed by ultrasonic disruption, and the supernatant was stained with 1× Gelstar (Cambrex Inc.) for 20 min before it was applied to the centrifugation tubes, where four sucrose density layers, i.e., 15%, 25%, 35%, and 45%, were mixed. Centrifugation was conducted at 160,000 × *g* for 4 h at 4°C. The AR particle bands displaying green fluorescence were located at about 35% sucrose density when checked with a blue diode DNA gel illuminator (Biovision, Xiamen, People's Republic of China). The collected AR from the staining band was dialyzed as described above and was also subjected to MALDI-TOF MS analysis.

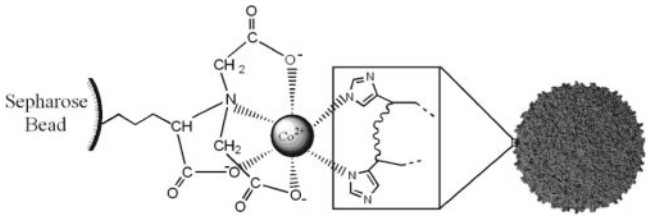

FIG. 1. Schematic illustration of the purification of His-tagged AR with a Co^{2+} affinity resin. Each AR assembly has 180 units of coat protein, and each coat protein has a His_6 tag exposed outward from the AR assembly, allowing chelated Co^{2+} on the resin beads accessibility to the His tag.

The concentration of AR particles purified through affinity chromatography was determined using the extinction coefficient of 0.125 mg/ml of MS2 bacteriophage per absorbance unit at 260 nm and a molecular weight of 3.0×10^6 (9).

AR purity test using real-time PCR. The purity of AR was checked by real-time PCR amplification of the cloned region with and without the reverse transcription step. Affinity-purified AR was lysed by heating at 95°C for 5 min and was then added to each PCR mixture. Each 30-μl RT-PCR mixture contained 5 μl lysed AR (~10^6 copies/ml), 10 mM Tris-HCl (pH 8.6), 50 mM KCl, 1.0 U *Taq*, 15 U Moloney murine leukemia virus reverse transcriptase, 30 U RNasin, 200 μM deoxynucleoside triphosphates, 2.0 mM $MgCl_2$, 0.4 μM each sense/antisense primer, and a molecular beacon probe. For SARS-CoV positive control detection, the primer pair was 5′-GCTCGCAAACATAACACTTGC-3′ and 5′-ACATATAGTGAGCCGCCACACATG-3′, and the probe was 5′–6-carboxyfluorescein (FAM)–CCGCACTACAGGTTAGCTAACGAGTGTGCGG–Dabcyl–3′. The primer pair for the internal control was 5′-CTGTTGTTAGACGACGAGG-3′ and 5′-GACTACAGACCACCAAATGC-3′, and the probe was 5′–6-carboxy-2′,4,4′,5′,7,7′-hexachlorofluorescein (HEX)–CCCAGGCATTCTTCGAGCTCATTCAAAACCTGGG-3′–Dabcyl. Real-time detection was performed using an iQ iCycler (Bio-Rad, Hercules, Calif.) started by RT for 1 h at 42°C (if included), followed by a denaturation step for 5 min at 95°C and 40 cycles of 15 s at 95°C, 20 s at 56°C, and 20 s at 72°C. The fluorescent signal was acquired at the annealing step.

Real-time RT-PCR detection of SARS-CoV. A single-step, dual-color, real-time RT-PCR optimized for SARS-CoV detection was carried out as follows. Each 50-μl reaction mixture contained 10 mM Tris-HCl (pH 8.6), 50 mM KCl, 1.0 U *Taq*, 15 U Moloney murine leukemia virus reverse transcriptase, 20 U RNasin, 200 μM deoxynucleoside triphosphates, 3.0 mM $MgCl_2$, 0.4 μM of each primer, 0.4 μM probes (primer and probe were the same as those described above), 0.2 μM of each primer for internal control AR, 0.2 μM of probe for internal control, and 10 μl template RNA (about 10^{10} copies). RT-PCR was started by reverse transcription at 42°C for 30 min, followed by 94°C for 5 min and 40 cycles of 30 s at 94°C and 30 s at 56°C. The purified AR positive control was 10-fold serially diluted to create a calibration curve.

SARS-CoV RNA from a variety of sources was extracted using RNA purification kits (BioVision, Xiamen, People's Republic of China). Internal control AR (5 μl, ~10^4 copies; this concentration was chosen due to its negligible influence on target amplification) was added to specimens before RNA extraction. Specimens include 17 confirmed patient samples (1 serum sample, 15 bronchoalveolar lavage fluid samples, and 1 stool sample) and 20 SARS-CoV-containing cell culture samples. All of the SARS-CoV-positive patient samples were confirmed for SARS-CoV infection by an immunofluorescence assay and enzyme-linked immunosorbent assay with a commercially available diagnostic kit (Beijing Genomics Institute, Beijing, People's Republic of China). In total, 100 negative serum samples collected from healthy blood donors were also included, and all these samples were confirmed to be negative by both immunofluorescence and enzyme-linked immunosorbent assays.

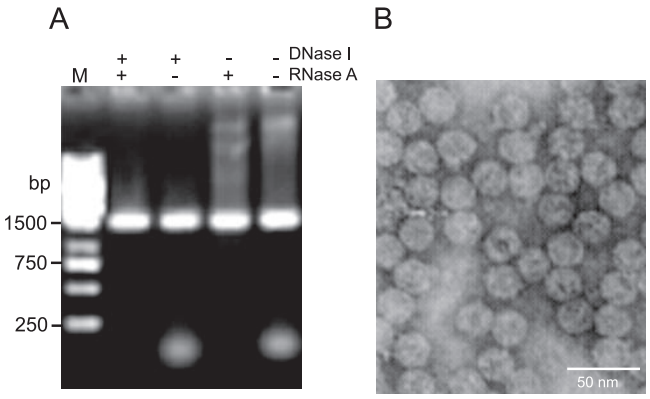

FIG. 2. Intact His-tagged AR assembly expressed in *E. coli*. (A) Agarose gel electrophoresis of AR treated (+) and not treated (−) with DNase I and/or RNase A. (B) TEM photograph of the His-tagged AR.

RESULTS

Production of His-tagged AR. AR inserted with a His tag between amino acids 15 and 16 of the MS2 coat protein was expressed in *E. coli* DH5α and purified by a Co^{2+}-nitrilotriacetic acid column. A schematic illustration of affinity purification of His-tagged AR is presented in Fig. 1. Unlike a common terminal His tag, the His insertion position in the AR was located at the central part of the β-hairpin loop of the coat protein that was exposed at the capsid surface and thus allowed the His tags accessibility to Co^{2+}. Like the MS2 bacteriophage, one AR assembly is composed of 180 coat protein monomers. Thus, there would be a total of 180 His tags displayed on the outside surface of each AR particle.

The existence of the intact His-tagged AR in the expression product was demonstrated by agarose gel electrophoresis, which showed a single band of about 1.5 kb of DNA (Fig. 2A) corresponding to the AR. Treatment with DNase I or RNase A did not affect the AR band intensity, while the bands for high-molecular-weight *E. coli* genomic DNA and cellular RNA disappeared after digestion. These results confirmed the production and packaging of RNA into the viral protein shell and the protective effect of the coat protein on the encapsulated RNA. A TEM photograph showed that the AR produced had the shape of a round particle that was 27 nm in diameter (Fig. 2B). This was consistent with MS2's icosahedral structure of the same size and further confirmed that the introduction of the His tag does not destroy the structure of the AR.

Purification of His-tagged AR. In order to keep the AR's integrity, we used nondenaturing conditions to purify AR. We tracked the purification procedure by using SDS-PAGE, which, however, showed the monomer of the coat protein in the denaturing environment. As shown in Fig. 3A, the His-tagged AR coat protein was captured by the resin (lane 3) and was eluted as a single band (lane 4). The molecular mass of the product shown was about 14.4 kDa, which is consistent with 1 unit of the coat protein. The exact molecular weight of the His-tagged coat protein was then measured with MALDI-TOF MS. The measured value of 14,739.15 (Fig. 3B) was consistent with the theoretical molecular weight of 14,739.89 calculated from the weights of the original coat protein (13,729.12) plus His_6 (155.09), one glycine (119.18), and one threonine (750.5) subtracted by that of $8\times$ H_2O. In comparison, the untagged coat protein purified by sucrose density gradient centrifugation showed a molecular weight of 13,728.87 (Fig. 3C), which is very close to its theoretical value of 13,729.12 as well.

The purity of affinity-purified AR. Following affinity chromatography, the quantity of AR was measured through absorption measurements. Usually, 1.0 mg of pure AR could be obtained with 2 ml fresh resin from 100 ml of cell culture. The RNA copy number was estimated through absorption measurements. To check whether there are any DNA contaminants in the AR preparation after affinity purification, both PCR and RT-PCR were performed. If there is any residual plasmid DNA contamination, both PCR and RT-PCR will produce an amplicon; otherwise, only RT-PCR will produce an amplicon. Our results showed that all affinity-purified AR controls produced robust RT-PCR signals but negligible PCR signals even in the presence of large amounts of AR (Fig. 4C). In contrast, unpurified AR (Fig. 4A) or AR purified by sucrose density gradient centrifugation (Fig. 4B) gave significant amplification signals with both RT-PCR and PCR procedures, indicating the existence of a large amount of plasmid DNA.

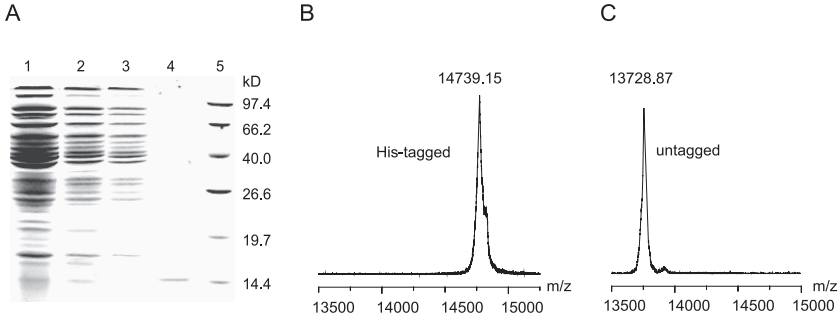

FIG. 3. Purification of the His-tagged AR and its molecular weight. (A) Different fractions of the affinity chromatography were run on an SDS-PAGE gel and stained with Coomassie brilliant blue R-250. Lane 1, supernatant of the cells lysate; lane 2, flowthrough solution; lane 3, first wash solution; lane 4, eluted solution; lane 5, marker. (B) MALDI-TOF MS of His-tagged and untagged coat protein. Affinity-purified AR was denatured by treatment with 10% β-mercaptoethanol at 95°C for 1 min. The precipitated protein was dissolved in 10 μl of 0.1% trifluoroacetic acid and purified with a Ziptip C_{18} column (Millipore, Shanghai, People's Republic of China). The eluted protein solution (1 μl) was mixed with matrix solution and then subjected to MALDI-TOF MS analysis.

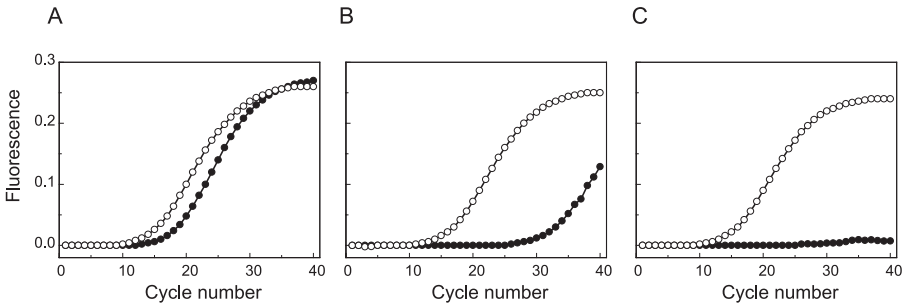

FIG. 4. Purity of AR verified with RT-PCR (empty circles) and PCR (solid circles). (A) Unpurified AR. (B) AR purified with sucrose density gradient centrifugation. (C) AR purified with Co^{2+} affinity chromatography.

The above-described results were confirmed by using many different preparations.

Real-time RT-PCR detection of SARS-CoV. According to the guidelines recommended by the WHO, we included both EPC and IPC for single-tube, dual-color, real-time RT-PCR detection of SARS-CoV. The AR EPC was used to establish a calibration curve for SARS-CoV quantification as well as for the evaluation of the overall performance of the assay. An IPC was included in the reaction mixture to monitor whether any potential inhibition occurred in the assay procedures. From the calibration curve, the limit of detection was determined to be 5 copies per assay. The calibration curve established with EPC concentration against cycle threshold (C_T) values showed no difference whether or not the internal control was included (Fig. 5A). Also, the C_T values of an internal control showed no change in the presence of different concentrations of EPC (Fig. 5B). These results demonstrated that EPC and IPC, when coexisting in one reaction tube, did not interfere with each other in an RT-PCR.

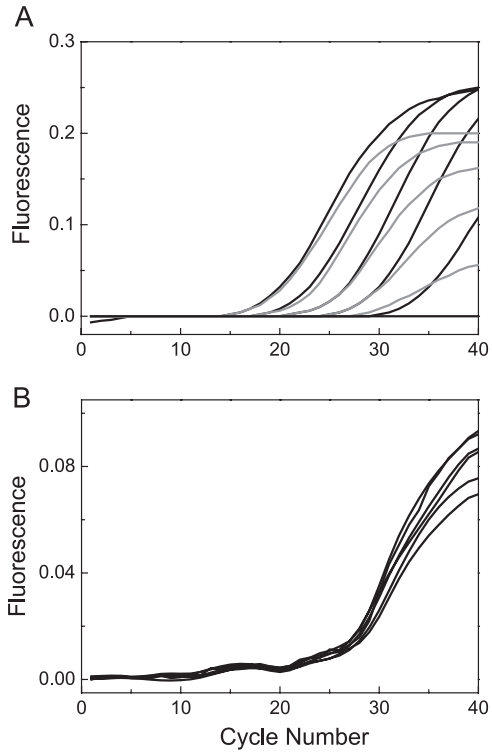

FIG. 5. Independent amplification of EPC and IPC in a single RT-PCR. (A) Real-time RT-PCR curves of AR EPC from 10^7 to 10^3 copies/ml (from left to right) in the absence (black line) and presence (gray line) of 10^4 copies/ml of IPC. Water was used as a negative sample. (B) Real-time RT-PCR curves of 10^4 copies/ml of AR IPC in the presence of different concentrations of EPC (from 10^7 to 10^3 copies/ml and 0 copies/ml).

SARS-CoV RNA from a variety of sources was detected using the above-described system. RT-PCR detected the presence of SARS-CoV RNA as reflected by the FAM fluorescence in all of the positive samples except the stool sample, while in all the negative samples, only HEX fluorescence was detected. In the case of the stool sample, neither HEX fluorescence (IPC) nor FAM fluorescence (target) was detected, suggesting that inhibition occurred. We then diluted the extracted RNA 10 times with water and repeated the assay; both HEX fluorescence and FAM fluorescence were detected. Clearly, the inhibition was correctly detected by the IPC. Together, all the results indicate that it is important to include the IPC for the SARS-CoV assay, especially for those samples containing potential inhibitors. The sensitivity and specificity of the assay based on the positive and negative specimens were calculated to be 100%.

DISCUSSION

The purity of AR is crucial when used as an RNA positive control and particularly as the standard for absolute quantification. Previous purification procedures involved tedious gradient ultracentrifugation plus size exclusion chromatography. In comparison, affinity chromatography is advantageous due to its simplicity and specificity. His tags are commonly used in recombinant protein purification (10); however, modification of the coat protein of AR presents unique challenges that must be overcome both mechanistically and operationally. Since the His tag has to be inserted into a specific site of the coat protein in order to present on the surface of the assembly, one risk is that the insertion may change the structure of the coat protein such that an intact MS2 particle could not be self-assembled (16a). We tried but failed to insert StrepTag or Tat into the same position, as no intact AR assembly was obtained. The successful affinity purification of AR would facilitate its wide applications as a positive control. Not only could extremely pure AR controls be obtained through single-step purification,

the preparation cost could also be lowered, as the Co^{2+} resin could be reused several times.

Although the inclusion of an IPC in nucleic acid-based testing is disputable (1, 12), we believe that an IPC should be mandatory at least for detection in clinical samples such as stool and urea and where inhibition most possibly occurs. This is in line with the guidelines recommended by the WHO for SARS-CoV detection. As observed in one case with the stool sample, the weak positive signal would have been missed had an IPC not been included.

Our results further demonstrated the advantages of noncompetitive IPC. The most attractive advantage is that noncompetitive IPC and the target could be independently amplified in the same reaction without interfering with each other. This advantage allows the sensitive detection of targets of low concentrations without competitive inhibition from IPC. It also allows the IPC to keep its C_T value unchanged at different target concentrations in real-time detection. Therefore, inhibition could be easily identified by simply measuring the C_T change of an IPC. In contrast, a competitive IPC may strongly inhibit the amplification of the target of low concentration and may even cause false-negative results (12). Moreover, the amplification of a competitive IPC was dependent on the target concentration and so was the C_T value of the IPC. Thus, the inhibition effect could not be identified by simply measuring the C_T change of the IPC, making it difficult, if not impossible, to be clarified when only a low level of inhibition occurs. An additional advantage of a noncompetitive IPC is that a universal noncompetitive IPC could be made for different targets, while a competitive IPC has to be made specifically for each target because the IPC and the target share the same primer pair. Recently, a natural MS2 bacteriophage was also proposed to be used as a noncompetitive IPC, which exhibited low variability when coamplified with the target gene (7). Nevertheless, an IPC made from AR could be detected in the presence of an EPC made from different AR and thus was more flexible than the native MS2 bacteriophage. We expected that affinity-purified AR would further facilitate its use as both an EPC and an IPC in RNA virus assays.

ACKNOWLEDGMENTS

We are grateful to Xilin Zhao for valuable comments on the manuscript.

This work was partially supported by the Natural Science Foundation of the Fujian Government (2003Y004), Xiamen Municipal Commission of Science and Technology Key Program, and Xiamen University Action Project.

REFERENCES

1. **Barkham, T.** 2004. Internal amplification control for PCR should not be mandatory in the clinical medical environment. J. Clin. Microbiol. **42:**3379–3380.
2. **Beld, M., R. Minnaar, J. Weel, C. Sol, M. Damen, H. van der Avoort, P. Wertheim-van Dillen, A. van Breda, and R. Boom.** 2004. Highly sensitive assay for detection of enterovirus in clinical specimens by reverse transcription-PCR with an armored RNA internal control. J. Clin. Microbiol. **42:**3059–3064.
3. **Bressler, A. M., and F. S. Nolte.** 2004. Preclinical evaluation of two real-time, reverse transcription-PCR assays for detection of the severe acute respiratory syndrome coronavirus. J. Clin. Microbiol. **42:**987–991.
4. **Brown, D., and B. L. Pasloske.** 2001. Ribonuclease-resistant RNA controls and standards. Methods Enzymol. **341:**648–654.
5. **Burkardt, H. J.** 2000. Standardization and quality control of PCR analyses. Clin. Chem. Lab. Med. **38:**87–91.
6. **Cartwright, C. P.** 1999. Synthetic viral particles promise to be valuable in the standardization of molecular diagnostic assays for hepatitis C virus. Clin. Chem. **45:**2057–2059.
7. **Dreier, J., M. Stormer, and K. Kleesiek.** 2005. Use of bacteriophage MS2 as an internal control in viral reverse transcription-PCR assays. J. Clin. Microbiol. **43:**4551–4557.
8. **Drosten, C., E. Seifried, and W. K. Roth.** 2001. TaqMan 5′-nuclease human immunodeficiency virus type 1 PCR assay with phage-packaged competitive internal control for high-throughput blood donor screening. J. Clin. Microbiol. **39:**4302–4308.
9. **Eisler, D. L., A. McNabb, D. R. Jorgensen, and J. L. Isaac-Renton.** 2004. Use of an internal positive control in a multiplex reverse transcription-PCR to detect West Nile virus RNA in mosquito pools. J. Clin. Microbiol. **42:**841–843.
10. **Gaberc-Porekar, V., and V. Menart.** 2001. Perspectives of immobilized-metal affinity chromatography. J. Biochem. Biophys. Methods **49:**335–360.
11. **Heal, K. G., H. R. Hill, P. G. Stockley, M. R. Hollingdale, and A. W. Taylor-Robinson.** 1999. Expression and immunogenicity of a liver stage malaria epitope presented as a foreign peptide on the surface of RNA-free MS2 bacteriophage capsids. Vaccine **18:**251–258.
12. **Hoorfar, J., N. Cook, B. Malorny, et al.** 2004. Diagnostic PCR: making internal amplification control mandatory. J. Appl. Microbiol. **96:**221–222.
13. **Hoorfar, J., B. Malorny, A. Abdulmawjood, N. Cook, M. Wagner, and P. Fach.** 2004. Practical considerations in design of internal amplification controls for diagnostic PCR assays. J. Clin. Microbiol. **42:**1863–1868.
14. **Konnick, E. Q., S. M. Williams, E. R. Ashwood, and D. R. Hillyard.** 2005. Evaluation of the COBAS hepatitis C virus (HCV) TaqMan analyte-specific reagent assay and comparison to the COBAS Amplicor HCV Monitor V2.0 and Versant HCV bDNA 3.0 assays. J. Clin. Microbiol. **43:**2133–2140.
15. **Liang, M. H., D. R. Johnson, and L. J. Wong.** 1998. Preparation and validation of PCR-generated positive controls for diagnostic dot blotting. Clin. Chem. **44:**1578–1579.
16. **Lion, T.** 2001. Current recommendations for positive controls in RT-PCR assays. Leukemia **15:**1033–1037.

16a. **Mastico, R. A., S. J. Talbot, and P. G. Stockley.** 1993. Multiple presentation of foreign peptides on the surface of an RNA-free spherical bacteriophage capsid. J. Gen. Virol. **74:**541–548.

17. **Pasloske, B. L., D. B. DuBois, D. M. Brown, and M. M. Winkler.** June 2002. Methods of quantifying viral load in an animal with a ribonuclease resistant RNA preparation. U.S. patent 6,399,307.
18. **Pasloske, B. L., C. R. WalkerPeach, R. D. Obermoeller, M. Winkler, and D. B. DuBois.** 1998. Armored RNA technology for production of ribonuclease-resistant viral RNA controls and standards. J. Clin. Microbiol. **36:**3590–3594.
19. **Peabody, D. S.** 2003. A viral platform for chemical modification and multivalent display. J. Nanobiotechnol. **1:**5.
20. **Reiss, R. A., and B. Rutz.** 1999. Quality control PCR: a method for detecting inhibitors of Taq DNA polymerase. BioTechniques **27:**920–926.
21. Reference deleted.
22. **Stocher, M., and J. Berg.** 2004. Internal control DNA for PCR assays introduced into lambda phage particles exhibits nuclease resistance. Clin. Chem. **50:**2163–2166.
23. **Stockley, P. G., and R. A. Mastico.** 2000. Use of fusions to viral coat proteins as antigenic carriers for vaccine development. Methods Enzymol. **326:**551–569.
24. **WalkerPeach, C. R., M. Winkler, D. B. DuBois, and B. L. Pasloske.** 1999. Ribonuclease-resistant RNA controls (Armored RNA) for reverse transcription-PCR, branched DNA, and genotyping assays for hepatitis C virus. Clin. Chem. **45:**2079–2085.
25. **Willhauck, M., S. Vogel, and U. Keilholz.** 1998. Internal control for quality assurance of diagnostic RT-PCR. BioTechniques **25:**656–659.